Soil Biology and Biochemistry 159 (2021) 108297

Contents lists available at ScienceDirect

Soil Biology and Biochemistry

journal homepage: www.elsevier.com/locate/soilbio

Belowground interplant carbon transfer promotes soil carbon gains in diverse plant communities

A.N. Kravchenko [a,b,*], H. Zheng [c], Y. Kuzyakov [d,e,f], G.P. Robertson [a,b,g], A.K. Guber [a,b]

[a] Department of Plant, Soil and Microbial Sciences, Michigan State University, East Lansing, MI, 48824, USA
[b] DOE Great Lakes Bioenergy Research Center, Michigan State University, East Lansing, MI, USA
[c] Research Institute of Agricultural Resources and Environment, Jilin Academy of Agricultural Science, Changchun, 130033, China
[d] Department of Agricultural Soil Science, University of Göttingen, Göttingen, Germany
[e] Institute of Physicochemical and Biological Problems in Soil Science, 142290, Pushchino, Russia
[f] RUDN University, Moscow, Russia
[g] W. K. Kellogg Biological Station, Michigan State University, Hickory Corners, MI, 49060, USA

ARTICLE INFO

Keywords:
X-ray computed micro-tomography
$^{13}CO_2$ pulse labeling
Prairie
Switchgrass
Big bluestem
Wild bergamot
Pore-size distribution
Soil pore architecture
Soil pore structure

ABSTRACT

Diverse plant communities are known to increase soil carbon (C) levels compared to monocultures, but an incomplete understanding of the underlying mechanisms of this phenomenon limits the development of strategies for optimizing soil C sequestration. We hypothesized that the identity of neighboring plants influences the amounts of C that a plant inputs into the soil, the resultant formation of soil pore architecture, and the fate of the plant's C inputs. To test this hypothesis, we combined $^{13}CO_2$ plant pulse labeling with X-ray computed micro-tomography (μCT) in assessing plant-assimilated C from three species common to North American prairie: switchgrass, big bluestem, and wild bergamot. The plants were grown in a greenhouse in monoculture and in all-pair combinations. The ^{13}C labeling was conducted so as to ensure that only one member of each pair has received ^{13}C. The results demonstrated that greater belowground C exchange among neighboring plants enhanced inputs of plant-assimilated C into soil, suggesting that the involvement of plant community members in belowground C transfer, rather than community's diversity per se, drives rapid soil C accrual. Moreover, the magnitudes of C losses as well as properties of soil pore architecture also depend not only on the identity of the C source plant itself but also on the identities of its neighbors. These findings propose belowground interspecific C transfer as a previously overlooked mechanism for enriching and stabilizing soil C and suggest genomic and management potentials for selecting species that participate in intensive interspecific assimilate exchange in order to promote rapid and stable soil C gains.

1. Introduction

Promoting C storage by soils is an important climate change mitigation strategy for reducing atmospheric CO_2 (Minasny et al., 2017; IPCC, 2018). Plant diversity is known to stimulate soil C accrual (Chen et al., 2020), particularly in native perennial grasslands (Cong et al., 2014; Kravchenko et al., 2019), but the underlying reasons remain poorly understood (Lange et al., 2015). Candidate mechanisms include, among others, greater root biomass (Cong et al., 2014), higher microbial biomass and activity (Tilman et al., 1996), and greater physical protection of accrued C (Kravchenko et al., 2019).

A key question is whether diversity-related C-sequestration stems from the presence of a certain species or a certain functional group within the plant community, e.g., C4 grasses, legumes, or deep rooting plants? Or is it produced by complementary interactions among species, so long as overall plant diversity is high (Tilman et al., 1996; van der Heijden et al., 1999)? In some perennial grasslands diverse plant systems outperformed any individual monoculture in promoting soil C accrual (Fornara and Tilman, 2008; Steinbeiss et al., 2008; Cong et al., 2015) and greater diversity per se resulted in greater soil C gains (Lange et al., 2015). Elsewhere, soil C gains were positively associated not so much with overall diversity but with the presence of different functional groups (Steinbeiss et al., 2008; Dawud et al., 2017; Yang et al., 2019) or a key species, for example *Trifolium pratense* (De Deyn et al., 2009,

Abbreviations: SW, switchgrass; BB, big bluestem; WB, wild bergamot; μCT, X-ray computed micro-tomography.

* Corresponding author. DOE Great Lakes Bioenergy Research Center, Michigan State University, East Lansing, MI, USA.
E-mail address: kravche1@msu.edu (A.N. Kravchenko).

https://doi.org/10.1016/j.soilbio.2021.108297
Received 4 March 2021; Received in revised form 24 April 2021; Accepted 5 May 2021
Available online 9 May 2021

2011). A better understanding of the basis for polyculture advantage could enable the design of crop- and grazing-land systems better able to accumulate and store soil C.

Switchgrass (*Panicum virgatum* L.) provides a case in point. As a dominant grass of North American prairies, switchgrass appears to readily contribute to soil C accrual as a member of diverse plant communities (Yang et al., 2019). But despite its extensive root system (McLaughlin and Kszos, 2005; Chimento et al., 2016), switchgrass can be slow to stimulate soil C gains when grown in monoculture (Kantola et al., 2017; Chatterjee et al., 2018). On the other hand, polycultures with switchgrass exhibit early C accrual (Sprunger and Robertson, 2018), likely related in part to the development of a soil pore architecture that favors rapid transfer of microbial metabolites and necromass to protective mineral surfaces or inaccessible micropores (Kravchenko et al., 2019).

We hypothesized that the identity of the neighbors with which switchgrass grows influences belowground C inputs and formation of pore architecture. The objective of the study was to test this hypothesis specifically focusing on (i) comparing belowground plant-assimilated C levels from switchgrass plants and its neighbors when grown in monoculture vs. in paired mixtures; (ii) exploring whether soil pore size distributions, which were developed during plant growth, are affected by the identities of the plants; and (iii) assessing losses of plant-assimilated C added to the soil shortly after plant termination.

We intercropped switchgrass (SW) with big bluestem (BB; *Andropogon gerardii*), another prairie grass known to be a positive contributor to soil C gains in diverse plant communities (Yang et al., 2019) but also in monoculture (Mahaney et al., 2008; Adkins et al., 2019), and with wild bergamot (WB, *Monarda fistulosa*), a prairie forb that commonly co-occurs with SW and BB. Plants were grown in different combinations for 3 months in a homogenized field-collected low-C soil with the majority of its inherent soil structure obliterated by sieving, thereby allowing plants to reveal their influence on spatial patterns of soil C accretion and soil pore architecture. We followed plant-assimilated C by pulse labeling in a $^{13}CO_2$ atmosphere and subsequent ^{13}C tracing, and tracked the formation of soil pore architecture using X-ray computed micro-tomography (μCT).

2. Materials and methods

2.1. Soil preparation

Surface soil (0–10 cm depth) was collected from a corn-soybean-wheat rotation within the Main Cropping System Experiment of the KBS Long-Term Ecological Research site, Hickory Corners, Michigan (lter.kbs.msu.edu). Soil texture is sandy loam (59% sand, 34% silt, and 7% clay), with total N and organic C equal to 0.07% and 0.75%, respectively, and soil pH of 5.7. Soil was air-dried and then ground to pass a 2 mm sieve. Small stones, visible roots, and plant residues were picked out during sieving and the sieved soil was rigorously mixed.

Greenhouse pots ~900 cm^3 in volume (10.5 × 10.5 cm (top), 8.5 × 8.5 cm (bottom), 10 cm tall) were filled with 1 kg of sieved soil to a bulk density of ~1.1 g cm^{-3}. The pots were watered to achieve 30% gravimetric water content prior to planting.

2.2. Plant treatments

Plant-assimilated C inputs to soil were evaluated with ^{13}C pulse labeling in a replicated blocked greenhouse experiment, where SW (var. Cave-in-Rock), BB, and WB were grown in all possible pairs with the same or another species (Fig. S1a). The roots freely shared the pot, but plants on only one side of the pot were subjected to $^{13}CO_2$ labeling (Fig. S1b). This allowed us to trace C from a source (^{13}C) plant to an unlabeled neighbor plant in both monoculture and intercropped combinations.

Each pot was planted either with seeds of the same species (referred to as monoculture) or with the seeds of one other species (polyculture), with each species planted to separate sides of a pot (Fig. S1a). Roots could freely intermingle in pots. The experiment consisted of a total of 10 experimental treatments: monocultures of each of the three species (SW, BB, WB), every pair of two species where the first member of the pair was labeled (e.g., a BB-WB mixture where BB was labeled and WB was unlabeled), every pair of two species where the second member of the pair was labeled (e.g., a WB-BB mixture where BB was unlabeled and WB was labeled), and an unplanted control. There were 5 replicated pots for each treatment. The seeds of the three studied species were purchased from Native Connections/Native Grass & Wildflower Seeds, MI. In preparation for planting, the seeds were subjected to acid scarification with 8 M sulfuric acid and then imbibed in a weak KNO_3 solution for 2 weeks at 4 °C.

A total of 8 seeds of each species were planted on each side of the pot. The seeds were covered by a thin layer (~2 mm) of a garden mix soil to prevent drying and enhance seed germination. During the entire experiment the pots were weighed daily, and water was added to each pot to maintain the soil water content level close to 0.3 g g^{-1}. The plants were fertilized using Hoagland's solution prior to planting and twice afterwards (approximately one and two months after planting). Approximately 2–3 weeks after germination only two plants were kept on each side of the pot – positioned so that they were approximately 3–5 cm away from each other. The rest of the plants were cut with scissors, and any subsequent regrowth, if occurred, was also promptly terminated. The pots were arranged in 5 replicated blocks within the greenhouse space, with pots within the block arranged in a random order.

2.3. ^{13}C pulse labeling

Labeling consisted of three 6 h pulses, one week apart. The labeling started when the plants were approximately 2 months old. At each labeling event the pots were moved into 80 × 60 × 60 cm air-tight glass chambers with ten pots of each replicated block placed within the same chamber (Fig. S1b). The chamber bases were placed in water filled trays to ensure airtightness. Prior to placing the pots in the chamber, a plastic frame was installed over the control (unlabeled) side of each pot and covered with a light-impermeable black plastic bag, taking care that all plants grown on the unlabeled side where within the bag and fully eliminating light access. We placed a container with 98% ^{13}C enriched $NaH^{13}CO_3$ solution (equivalent to 88 mg ^{13}C released per pulse event per chamber) in the middle of each chamber. The container was connected via plastic tubing to a syringe with H_2SO_4 solution. An electric fan, placed next to the $NaH^{13}CO_3$ container, ensured free circulation of evolving $^{13}CO_2$. A thermometer and PYR Pyranometer (METER Group, Inc., Pullman, WA, USA) installed inside the chamber monitored air temperature and measured solar radiation, respectively. Selected chambers were outfitted with tubes for air sampling and connected to an infrared Photoacoustic Spectroscopy (PAS) (1412 Photoacoustic multigas monitors; INNOVA Air Tech Instruments, Ballerup, Denmark), which enabled CO_2 levels within the chamber to be monitored during labeling. At the start of each labeling event 10% H_2SO_4 was added in excess to react with $NaH^{13}CO_3$. CO_2 concentrations within the labeling chambers reached maximum of ~1200 ppm approximately 6 h after the start of the labeling.

During each labeling event the plants remained within the chamber for 6 h. Temperature within the chambers was monitored and ice was added as needed to the outsides of the chambers to ensure that air temperature stayed within a 25–30 °C range (Fig. S1b). Then the plants were taken out of the chambers, the black covers were removed, and the plants were kept in a well-ventilated area under daylight lamps for another 12 h to promote further photosynthetic activity. After the last pulse event the plants grew for another week and then harvested.

2.4. Plant and soil sampling

The plants were cut with scissors at the crown level, placed in paper bags and dried in an oven at 30 °C to constant weight. Aboveground biomass of plants on each side of the pot was processed and measured separately. Aboveground biomass for ^{13}C analyses consisted of composite samples taken from representative portions of top, mid, and bottom parts of each plant.

Two intact soil micro-cores (0.8 cm Ø and ~2 cm height), were taken from the labeled sides of the pots at distances of ~3 cm from the center of the pot and at ~1 cm distance from the pot corners (Fig. S1c). The micro-cores were taken from 0.5 to 2.5 cm depth. One of the two cores was then randomly selected for subsequent incubation and μCT scanning.

After soil micro-core collection, the roots were carefully separated from soil, taking care to trace individual roots to plant crowns on labeled vs. unlabeled sides of the pots. A minor portion (<20%) of root material was not unequivocally ascribed to a specific side of the pot and treated separately. After initial separation, the roots were washed of remaining soil and dried at 30 °C. Belowground biomass for ^{13}C analyses was taken from three separate plant parts: crown of individual plants, coarse roots (~2–3 mm in diameter) connected to a crown, and fine root (<1 mm in diameter) connected to coarse roots. Throughout sampling we ensured that sampled roots belonged to the plants grown either on the labeled or on the unlabeled side of the pots.

Loose soil obtained after intact soil sampling and initial root separation was collected, carefully mixed with visible root pieces removed, placed in plastic bags to prevent drying, and stored at 4 °C until further analyses. A 20 g sub-sample was taken for soil ^{13}C analysis, well mixed, further cleaned from any visible root residues, and air-dried. From each pot we used 2–5 laboratory replicates for soil ^{13}C analyses.

^{13}C analysis was conducted using an elemental analyzer (Vario ISOTOPE CUBE, Elementar Americas Inc., Ronkonkoma, NY) coupled to an isotope ratio mass spectrometer (Isoprime Vision, Elementar Americas Inc., Ronkonkoma, NY). The ^{13}C enrichment data are reported as $\delta^{13}C$ (‰) and as the total ^{13}C contents for the labeled plants and for the soil. To quantify the ^{13}C enrichment of the labeled plants and soil the absolute isotope ratios ($^{13}C/^{12}C$) were obtained based on the PeeDee Belemnite standard, then the ^{13}C atom% excess was calculated by subtracting ^{13}C atom% in the non-labeled plants and control soil, and the total ^{13}C contents in the plant and soil was calculated by accounting for their respective C levels and the total weights.

2.5. Soil pore characterization with μCT

A total of 30 air-dried micro-cores, one randomly selected micro-core per pot for 3 replicates of each treatment, were used to characterize soil pores. The cores were scanned on the bending magnet beam line, station 13-BM-D of the GeoSoilEnviroCARS at the Advanced Photon Source, Argonne National Laboratory (Lemont, IL USA). The energy of the monochromatic beam was 24 keV, and the scanning resolution was 5.7 μm. The reconstructed three-dimensional image consisted of 850 slices with 1920 × 1920 pixels per slice, covering approximately 5 mm of the micro-core's height. The μCT image analyses were conducted using ImageJ/Fiji (Rasband, 1997–2015). The original images were pre-processed using a 3D Gaussian blur filter with a 3 × 3 × 3 pixel window followed by 3D contrast enhancement. Image segmentation into solids and pores was conducted using the Renyi Entropy segmentation procedure available in ImageJ (Kapur et al., 1985). Image-based porosity was obtained as the ratio of the voxels occupied by all pores visible at the image resolution (≥5.7 μm) to the total number of the image voxels. Separation of pores into size classes was conducted using the continuous 3D pore-size distribution determination approach of Xlib plugin for ImageJ (Munch and Holzer, 2008). The pore size at a specific location was defined by the software as the radius of the maximally inscribable sphere at this location.

While the roots were initially selected by visual examination of the gray-scale images, their exact identification occurred via thresholding. Thresholding was conducted using manually pre-selected lower and upper boundaries of gray-scale values typical for the roots (Fig. S2a). However, besides identifying the inclusions, the thresholding also produced partial volume effect artifacts, primarily on boundaries of soil solids and pores (Fig. S2b). To remove artifacts we identified such boundaries using the Find Edges tool, and then thresholded and removed the edges. Several 3D Erode steps were applied to remove any remaining large artifacts, followed by Particle Analyzer of BoneJ (Doube et al., 2010) to separate the inclusions from lingering artifacts. Upon segmentation, roots were excluded from pore-size distribution analysis.

2.6. Incubation of soil mini-cores

For the incubation, the micro-cores were brought to a 50% water filled pore space and placed into 480 mL Mason jars holding a small container with water to reduce evaporation from the soil. At the end of a 10-day incubation period, gas samples (5 cm^3) were taken from each jar for $^{13}CO_2$ and CO_2 analyses.

2.7. Statistical analysis

Comparisons among the studied plant systems were conducted using a mixed model approach (Stroup et al., 2018). The fixed effects of the fitted statistical models differed depending on the response variable. The statistical model for the aboveground and belowground plant biomasses and for the aboveground ^{13}C level consisted of the fixed effects of the plant system and the labeling treatment and their interactions. The statistical model for the belowground ^{13}C level consisted of the fixed effects of the plant system, the labeling treatment, the plant root component (fine root, coarse root, and crown), and their interactions. All statistical models for comparisons among the studied plant system treatments included the random effects of experimental blocks and pots. Pots were specified as nested within the blocks and plant systems and were used as error terms in testing the plant system effects. The random effect of the labeling treatment interaction with the pot was used as an error term for testing the effect of the labeling. The differences among the labeled plant systems in terms of pore-size distributions were assessed using repeated measures analysis. The micro-core, nested within the plant system, was used as an error term for testing the plant system effect and as a subject of repeated measures analyses. The mixed model analyses were conducted using PROC MIXED and PROC GLIMMIX procedures in SAS (Stroup et al., 2018). Correlation and simple linear regression analyses were conducted using PROC CORR and PROC REG procedures in SAS.

In all analyses the normality of the residuals was assessed by visual inspection of normal probability plots. The homogeneity of variance assumption was first assessed by visual examination of side-by-side box plots of the residuals followed by the Levene's test for unequal variances. When assumptions were found to be violated the data were either square-root- or log-transformed as needed to achieve normality or the unequal variance analysis was performed (Milliken and Johnson, 2009).

When the plant system effect was statistically significant ($p < 0.05$), comparisons among the systems were conducted either using all-pairwise comparisons with t-tests or using the contrasts to compare the specific combinations of the plant system means, reflecting the pre-planned treatment structure of the study. Among the examples of such comparisons are differences between the plant systems with the same plant combinations, regardless of which plant was labeled, or differences between the plant systems with the same ^{13}C source plant. Differences significant at $p < 0.1$ level were reported as trends.

a) The ^{13}C source plant is switchgrass (SW). Red, blue, and green represent SW-SW, SW-BB, and SW-WB systems, respectively.

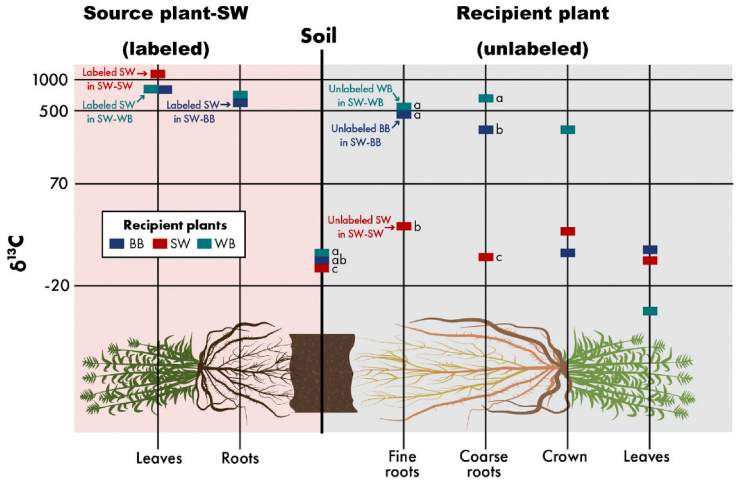

b) The ^{13}C source plant is big bluestem (BB). Blue, green, and red represent BB-BB, BB-WB, and BB-SW systems, respectively.

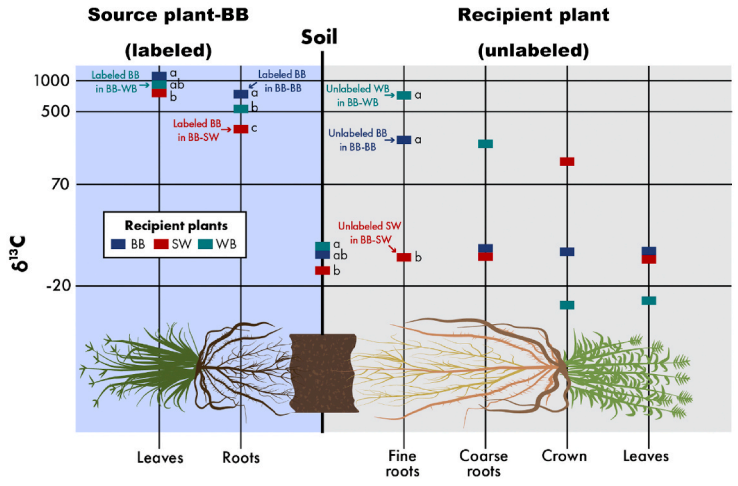

c) ^{13}C source plant is wild bergamot (WB). Green, blue, and red represent WB-WB, WB-BB, and WB-SW systems, respectively.

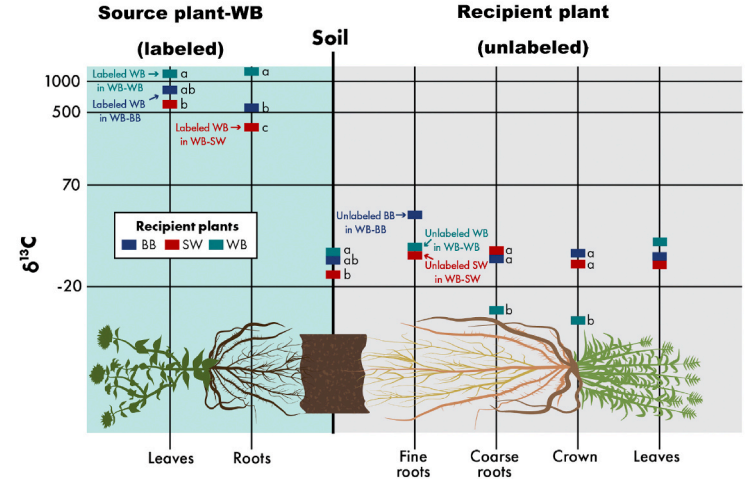

Fig. 1. Median values for $\delta^{13}C$ in a progression from the labeled plants to the soil and further to the unlabeled plants. Results are grouped by labeled/source plants: **a)** switchgrass (SW), **b)** big bluestem (BB), and **c)** wild bergamot (WB). Colors represent the unlabeled neighbor plants that were grown in pairs with the source plant. Letters mark significant differences among neighbor plants within each studied material, no letters are shown when the differences were not statistically significant ($p < 0.05$). . (For interpretation of the references to color in this figure legend, the reader is referred to the Web version of this article.)

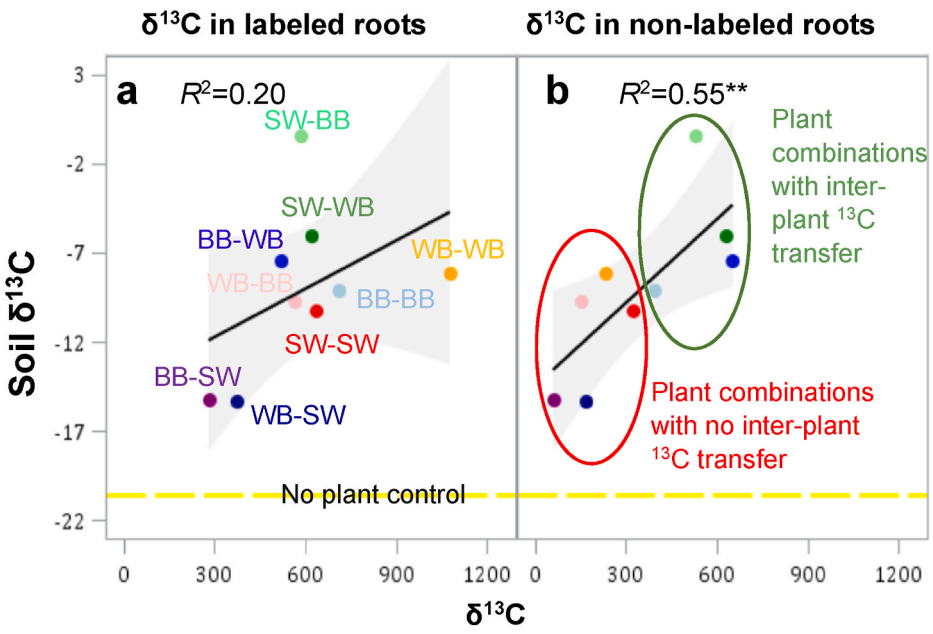

Fig. 2. Soil $\delta^{13}C$ values of the plant systems plotted as a function of the ^{13}C levels in roots. **a)** $\delta^{13}C$ in the roots of the labeled plants and **b)** $\delta^{13}C$ in the fine roots of the unlabeled neighbor plants. Plant combinations are identified by colors and text labels where the first and second parts stand for the labeled and non-labeled plants, respectively: SW, switchgrass; BB, big bluestem; WB, wild bergamot. Shown are averages (n = 5). Yellow dash line marks the unplanted control soil. ** mark the R^2 significant at $p < 0.05$, shaded area represents 95% confidence intervals for the mean. (For interpretation of the references to color in this figure legend, the reader is referred to the Web version of this article.)

3. Results

3.1. Interplant and plant-soil transfers of photo-assimilated C

SW grown with WB and BB had higher aboveground biomass than other systems (Fig. S3a). The two grasses, BB and SS, had higher belowground biomass than WB (Fig. S3b).

Inter-plant transfer of the assimilated ^{13}C was readily observed: median $\delta^{13}C$ in fine roots of the unlabeled neighbors was equal to 89‰. Approximately 40% of the unlabeled neighbors had $\delta^{13}C$ in their fine roots exceeding 200‰. $\delta^{13}C$ signatures of the aboveground biomass of the unlabeled neighbors were never elevated (Fig. 1) excluding possibility of plant contamination during labeling pulses.

Transfer was strongly species and neighbor dependent (Fig. 1). ^{13}C from SW source plants was observed in both fine and coarse roots of BB and WB unlabeled neighbors, but there was no detectable ^{13}C transfer from SW sources to SW neighbors (Fig. 1a). Likewise, while ^{13}C was transferred from BB source plants to the fine roots of WB and BB neighbors, there was no detectable transfer from BB to SW (Fig. 1b). Labeled WB did not transfer ^{13}C to any of its unlabeled neighbors (Fig. 1c).

Soil was ^{13}C enriched (Fig. 1) and, as might be expected (Remus and Augustin, 2016; Loeppmann et al., 2019), greater $\delta^{13}C$ levels in the soil were associated with greater total ^{13}C levels in the roots of the source plants (Fig. S5). However, $\delta^{13}C$ in the roots of the source plants was not a good predictor of soil $\delta^{13}C$ (Fig. 2a). Surprisingly, soil $\delta^{13}C$ was much better predicted by $\delta^{13}C$ in the fine roots of the unlabeled neighbors (Fig. 2b), which explained 55% of variability in soil $\delta^{13}C$ values. This result suggests that the more C passed-by via interplant transfer the more of it remained in the soil. With one exception, the plant systems with interplant C transfer (source-neighbor: SW-WB, SW-BB, BB-WB, and BB-BB) had higher soil $\delta^{13}C$ signatures than the systems with

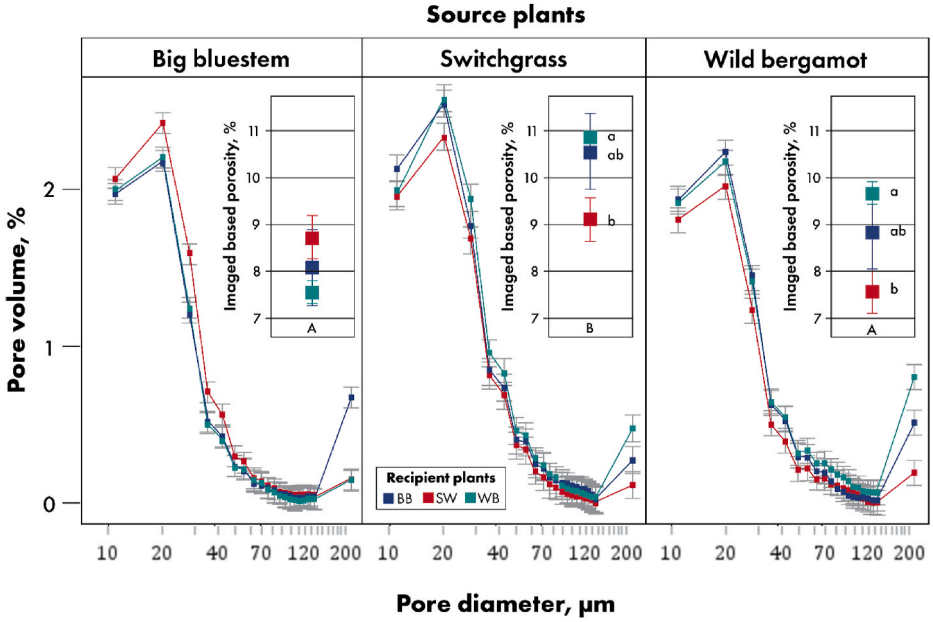

Fig. 3. Soil pore characteristics in vicinity of source plants. Panels represent the ^{13}C source plants. Colors mark the unlabeled neighbor plants. The intact soil mini-cores used in the analyses were taken from the sides of the pots that were accessible primarily by the roots of the source plants, but not by the roots of the neighbor plants. **Main graph:** Pore size distributions for >10 μm Ø pores determined from μCT images of the intact soil cores. **Insert:** Image-based porosity, i.e., total volume of >10 μm Ø pores. Shown are means and standard errors (n = 3). Low-case letters indicate statistically significant differences among the unlabeled neighbor plant treatments within each source plant group ($p < 0.05$). Upper-case letters mark the significant differences among t he source plants across the unlabeled neighbor groups ($p < 0.05$). (For interpretation of the references to color in this figure legend, the reader is referred to the Web version of this article.)

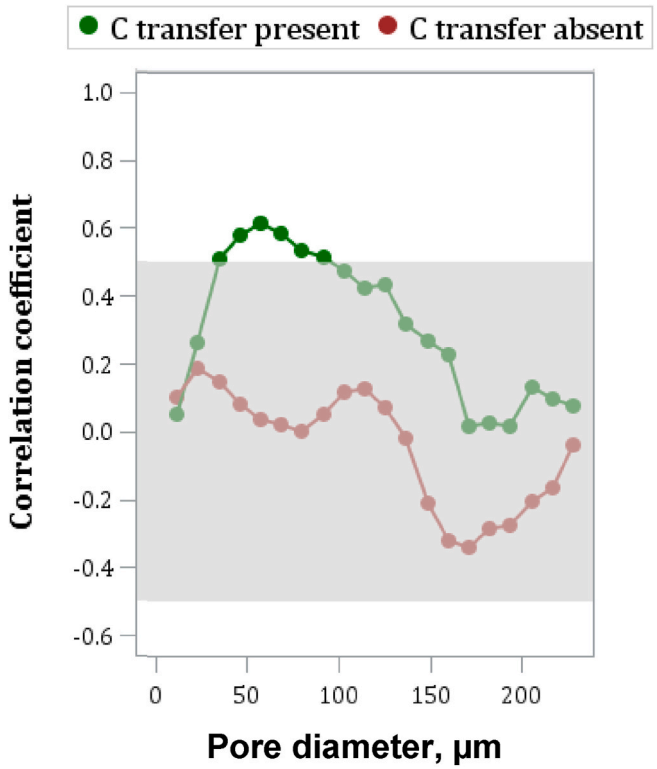

Fig. 4. Correlation coefficients between $\delta^{13}C$ in the fine roots of unlabeled neighbor plants and the volumes of pores with diameters ranging from 10 to 250 µm in plant systems with and without substantial interplant C transfers. Circles represent correlation coefficients. For each correlation coefficient the numbers of observations are equal to either 12 or 15 for the data from the C transfer present or the C transfer absent groups, respectively. Shaded gray area marks the range of correlation coefficient values that are not significantly different from zero, ~ from −0.5 to 0.5 ($p < 0.05$).

negligible transfer (WB-BB, WB-SW, BB-SW, SW-SW). The exception was WB-WB, where soil $\delta^{13}C$ was relatively high even though no noticeable interplant C transfer occurred, perhaps reflecting exceptionally high $\delta^{13}C$ in WB source roots (Fig. S4b).

3.2. Effects on soil pore characteristics

Three months of plant growth generated soil pore characteristics consistent with the observed accumulation of ^{13}C in soil. Intact soil micro-cores (8 mm Ø) from the immediate vicinity of ^{13}C source plants (Fig. S1c) showed species-specific differences in total volume of >10 µm Ø pores, i.e., image-based porosity (Fig. 3 insert). The abundance of pores in specific size groups (Fig. 3 main) also differed by source plant. Soil near SW source plants had greater image-based porosity than soil near BB and WB source plants for all recipient plants (Fig. 3 insert) and had a higher abundance of small (10–60 µm Ø) but not large (>60 µm Ø) pores (Fig. 3 main). The higher root density of SW was one of the expected contributors to the higher porosity (Bodner et al., 2014; Poirier et al., 2018), but overall, the observed trends in root densities were not consistent with the trends in pore characteristics (Fig. S3b).

Surprisingly, the identity of the neighbor plant also influenced pore characteristics observed near the ^{13}C source plants. Soil near WB and SW source plants had significantly higher image-based porosity and a higher abundance of 20–40 µm Ø pores when WB and, to a lesser extent, BB were their neighbors as compared to SW neighbors. In all three source plant systems (SW, BB, and WB) the abundances of >200 µm Ø pores differed depending on neighbors, and, with one exception (low >200 µm Ø pores in BB-WB system), the volumes of such pores were lower in the systems with SW neighbors.

3.3. Associations between soil pores and inter-plant C transfer

In the systems with interplant C transfer (SW-BB, SW-WB, BB-WB, BB-BB), pore volumes were significantly positively associated with $\delta^{13}C$ in the fine roots of unlabeled neighbor plants for pores in the ~35–80 µm Ø range (Fig. 4). In the systems with negligible interplant C transfer (BB-SW, WB-SW, SW-SW, WB-WB), there were no significant correlations between the $\delta^{13}C$ signature of unlabeled plants and pores of any sizes.

3.4. Does C from interplant C transport persist in soil?

We measured total CO_2 and $^{13}CO_2$ respired from decomposing rhizodeposits in micro-cores incubated for 10 days. Total amounts of emitted CO_2 did not differ among systems (Fig. 5a). But the systems with negligible interplant C transfer (BB-SW, WB-SW, SW-SW, WB-WB) emitted almost two times more $^{13}CO_2$ than did the systems with C transfer: 0.23 vs. 0.12 mg ^{13}C lost per mg of ^{13}C in labeled roots,

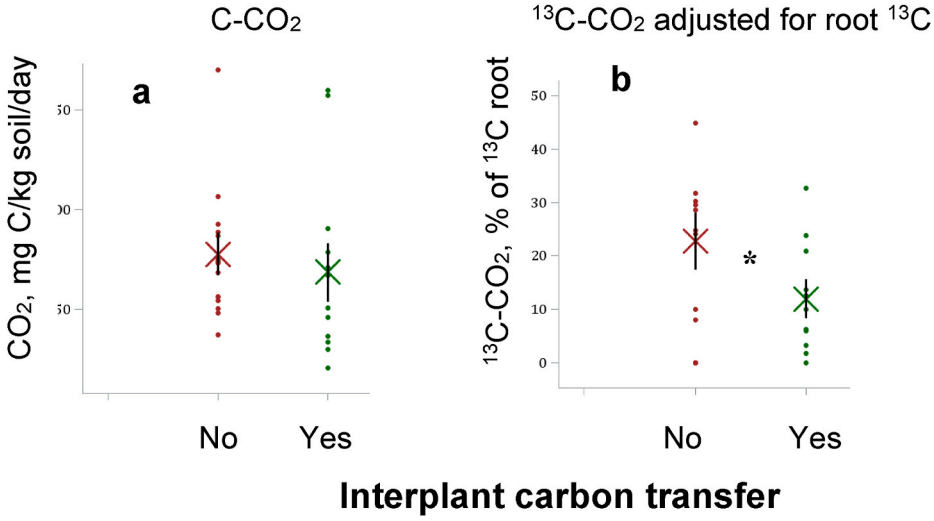

Fig. 5. Carbon losses from the soil in vicinity of source plants. The total amount of CO_2 released after 10-day incubation **(a)**, and the released ^{13}C–CO_2 adjusted for the total amount of ^{13}C present in the roots within the samples **(b)** from the plant systems with and without presence of C transfer. Shown are individual data points, means (X) and standard errors for the means (vertical black lines). * mark statistically significant difference between the two groups ($p < 0.1$).

respectively (Fig. 5b).

4. Discussion

Our findings suggest that interplant C transfer, rather than plant diversity per se, is one of the drivers of rapid soil C accrual. Plant combinations stimulating C transfer generated the highest soil $\delta^{13}C$ signatures. Switchgrass demonstrated sizeable interplant C transfer only in polyculture, but not in monoculture (Fig. 1a). This result explains a seeming contradiction between prior reports of slow soil C gains in monoculture SW (Kantola et al., 2017; Chatterjee et al., 2018) and the reports of the positive role that SW plays in stimulating soil C accrual in diverse plant communities (Yang et al., 2019). Big bluestem demonstrated interplant C transfer in both monoculture and polyculture (Fig. 1b). This result is consistent with prior reports showing that monoculture BB supplies higher amounts of plant-assimilated C to the soil than monoculture SW (Adkins et al., 2019), and generates higher overall soil C gains than SW; the results obtained in multi-year field experiments (Mahaney et al., 2008; Adkins et al., 2019).

Interplant C transfers can occur via mycorrhiza mycelia shared among neighbor plants (Francis and Read, 1984) and via root uptake of exudates originated from neighbor plants. The latter can occur either directly, when roots of different plants intermingle, or indirectly, after root exudates undergo microbial processing (Newman and Ritz, 1986). Interplant transfers facilitated by common mycorrhizal networks of both arbuscular and ectomycorrhizal fungi are well-known for enabling nutrient and water exchange among plants (Simard et al., 1997, 2012). All three studied plant species, i.e., BB, SW, and WB, form mycorrhizal associations (Johnson et al., 2015; Emery et al., 2018; Jach-Smith and Jackson, 2018, 2020). Nitrogen is the resource most often transferred among plant species via common mycorrhizal networks (Meding and Zasoski, 2008; Montesinos-Navarro et al., 2017). In such transfers, the resource flow generally follows a gradient from plants with higher to those with lower levels (Montesinos-Navarro et al., 2017). N and C transfers can occur jointly since N is often transported as amino acids (Smith and Smith, 2011). Likewise, in a course of non-mycorrhizal C transfers plants can uptake simple organic compounds directly, including amino acids and polyamins (Jones et al., 2009), thus getting C along with the target N.

The greatest interspecific C transfers in our experiment took place from SW sources to BB and WB unlabeled neighbors (Fig. 1a), while transfers to SW from any sources, including other SW, were negligible (Fig. 1a, b and 1c). Switchgrass is known for its associative N fixation capabilities (Roley et al., 2018; Smercina et al., 2019) as well as for procuring N through its mycorrhizal associations (Jach-Smith and Jackson, 2018). BB may also host associative N fixers (Weaver et al., 1980) and is known to transfer nutrients to prairie forbs (Walter et al., 1996). In the N deficient soil of our experiment, associative N fixation under SW could have made it an N-source for other plants, facilitating transfer of N and of C along with it. Our finding of greater ^{13}C transfers from SW and BB to WB (Fig. 1) is consistent with the notion that interspecific transfers tend to favor species that are distantly related to each other rather than among close relatives (Montesinos-Navarro et al., 2017).

Soil C gains appear to result from the loss of plant-assimilated C during its transfer to recipient neighbors (Newman and Ritz, 1986; Jones et al., 2009). While results here cannot identify the mechanism primarily responsible for ^{13}C soil inputs, we note that plant-assimilated C transported via mycorrhizal hyphae can be three times greater than transport via the indirect soil pool route (Philip et al., 2010). Carbon from hyphae can enter the soil pool when released by the fungi to support other beneficial microbes (Kaiser et al., 2015), upon hyphae consumption by other (micro)organisms, and upon senescence (Staddon et al., 2003). Microorganisms can be expected to out-compete plant roots for labile organic compounds (Jones et al., 2009; Fischer et al., 2010), so non-mycorrhizal C transfer likely results in a substantial loss of C to microbial communities (Jones et al., 2005; Moran-Zuloaga et al., 2015).

It is well known that plant species differentially affect soil pore architecture due to differences in root characteristics (Materechera et al., 1992; Helliwell et al., 2019). Intra- and inter-species competition among the plants can lead to modifications in their root traits and the amounts of rhizodeposits they produce (Schenk, 2006; Sanaullah et al., 2012; Sun et al., 2020). Our results for the first time experimentally demonstrated that not only the identity of the plant itself, but also the identity of its neighbors can affect the plant's contribution to pore formation. Pore architecture is an important factor affecting soil C accrual and subsequent protection (Kravchenko et al., 2019) and our findings suggest that judicious selection of species for inter-cropping could enhance the development of pore architecture conducive to soil C sequestration.

Organic inputs from roots (Naveed et al., 2017; Poirier et al., 2018) and promotion of mycorrhizal fungal networks (Rillig and Mummey, 2006; Leifheit et al., 2014) were likely the main mechanisms of differentially enhanced pore formation in our experimental systems. Organic compounds released by roots influence pore formation directly by acting as a gluing agent that connects and then consolidates soil particles upon drying (Tisdall and Oades, 1982; Horn et al., 1994), as well as indirectly by stimulating microbial activity (Chenu and Cosentino, 2011). During plant growth, a sequence of recurring organic inputs, accompanied by spatially variable wetting and drying events due to localized root water uptake, results in anisotropic soil shrinkage, consolidation, and aggregation of particles (Chenu and Cosentino, 2011; Carminati et al., 2013; Helliwell et al., 2017), and leads to formation of pores in a hierarchy of sizes. Microbial activity, enhanced by new inputs within the rhizosphere, detritusphere, and surrounding soil (Strong et al., 2004; De Gryze et al., 2006; Feeney et al., 2006), further redistributes the organic compounds through the soil matrix. Microbial products serve as additional gluing agents, as, for example, glucoproteins and other compounds produced by mycorrhizae (Chenu, 1989; Rillig et al., 1999). Inputs of organic compounds from both living and decomposing hyphae stabilize and enlarge the initially small, few-micron diameter, pores (Dorioz et al., 1993; Bearden, 2001; Emerson and McGarry, 2003). These multifaceted contributors modify the entire pore-size distribution, including very small pores (Milleret et al., 2009).

The positive associations between interplant C transfer, i.e., $\delta^{13}C$ in fine roots of unlabeled plants, and pores in the ~35–80 μm Ø size range (Fig. 4) are consistent with a potential mycorrhizal C transfer. Pores of this size are barely accessible to the finest roots (~40 μm Ø) but are readily accessible to root hairs (~10 μm Ø) (Gahoonia et al., 1997; Grierson et al., 2014) and fungal hyphae (2–20 μm Ø) (Smith and Smith, 2011). Fungi can contribute to the formation of these pores by providing organic inputs, as mentioned above, and also by physically binding and rearranging soil particles (Tisdall and Oades, 1982; De Gryze et al., 2006). While observed associations cannot prove cause-effect, it seems safe to conclude that pores of this size range either experienced greater development during interplant C transfer, or served as fungal routes for such transfer, or both.

While a 10-day incubation conducted in this study is too short to infer long-term persistence, results indicate a potential for interplant C transfer contributing to longer term C sequestration (Fig. 5). Plant species are known to differ in their roles in decomposition of resident soil organic matter as well as in processing labile C additions (Carrillo et al., 2017); and inter-species competition can influence rhizosphere priming (Pausch et al., 2013). Our results suggest that the magnitudes of differences among individual species and polyculture communities in protection of newly added photo-assimilates might depend on the presence of inter-plant C transfers during plant growth.

Soil organic C and pore characteristics are closely linked within a feedback cycle: greater accumulation of organic matter leads to development of heterogeneous pore structure and aggregate formation (Tisdall and Oades, 1982). While soil texture and mineralogical composition can greatly mediate the interactions between pore structure and C protection, in most soils greater pore heterogeneity and greater

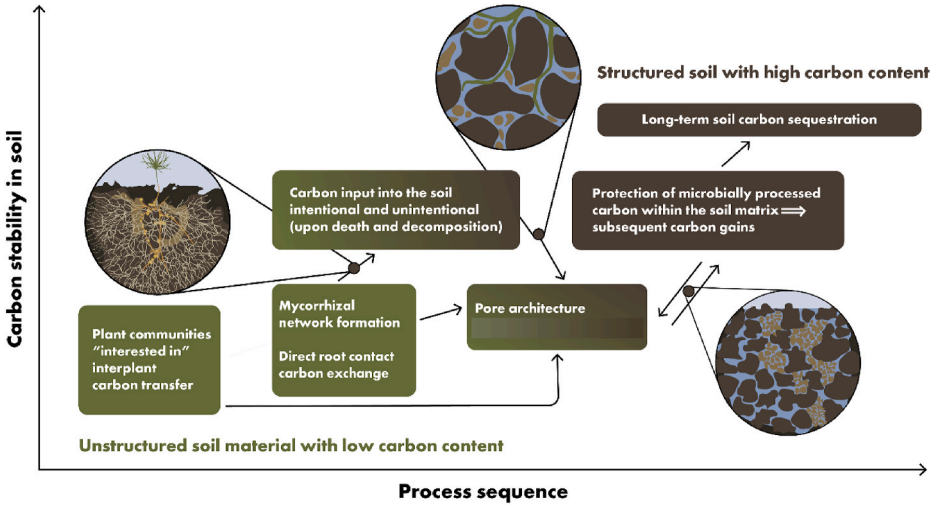

Fig. 6. Conceptual model of temporal sequence in interplant C transfer contributions to soil C gains. Presence of plant community members, which can benefit from interplant C transfer (e.g. because of N deficiency, light deficiency, etc.) is the starting point of the process. Mycorrhizal networks are likely the main routes of the transfer, however, exchanges through direct root contacts might play a role as well. The portion of the C that was intended for the interplant transfer but has not reached the recipient plant is microbially processed and microbial decomposition products are entombed within the soil matrix. That further stimulates development of heterogeneous pore structure, starting a feedback cycle of greater soil C → greater pore structure development → greater C protection and further C gains.

aggregation, in turn, boost protection of soil C and promote C gains (Six et al., 2000). Mycorrhizal fungi play an important role in this process both as conduits of plant-assimilated C into the soil and as drivers of soil structure formation (Wilson et al., 2009). Our results identify the starting point of this cycle in diverse plant communities –i.e., enhanced plant-assimilated C inputs stimulated by interplant C transfers via, among other mechanisms, mycorrhizal fungi networks, which subsequently encourage pore formation (Fig. 6).

In conclusion, we would like to emphasize that these findings help to explain the apparent inconsistency between slow C gains and poorly developed pore structure in monoculture switchgrass as compared to fast C gains and well developed pore structure in diverse prairie communities which include switchgrass (Kravchenko et al., 2019; Yang et al., 2019). Our results suggest that interplant C transfer within diverse plant communities is important for enabling early C gains from rhizosphere C leakage and the subsequent development of a pore architecture, which in the studied soil was beneficial for further C protection and sequestration (Fig. 6). That said, it is also clear that some plant species are more capable than others for enriching soil with plant-assimilated C via either interplant intraspecific transfers, as for big bluestem in this study, or intra-plant C transfer to the roots, as for wild bergamot. A better understanding of interspecific differences in interplant C transfers and their consequences for soil physical attributes could provide a means to design plant communities – and plants – that better promote stable soil C accumulation.

Author contributions

A.N.K. developed research concepts with inputs from A.K.G, G.P.R., and Y.K.; H.Z. conducted the experimental work; A.N.K. and A.K.G. conducted data analyses; A.N.K. and G.P.R. wrote the manuscript. All authors contributed to manuscript writing and reviewed the manuscript.

Declaration of competing interest

The authors declare that they have no known competing financial interests or personal relationships that could have appeared to influence the work reported in this paper.

Acknowledgements

We are indebted to Maxwell Oerther for running and organizing greenhouse experimentation and laboratory analyses, to Kyungmin Kim and Weiqing Zhang for assistance with greenhouse work, and to Nick Candela for assistance with sample processing. We would like to thank Chelsea Mamott for the artwork and GLBRC communication team for help with figure preparations.

This research was funded by the NSF DEB Program (Award # 1904267), by the NSF LTER Program (DEB 1027253) at the Kellogg Biological Station, and by the Great Lakes Bioenergy Research Center, U. S. Department of Energy, Office of Science, Office of Biological and Environmental Research under Award Number DE-SC0018409, and by Michigan State University AgBioResearch.

Appendix A. Supplementary data

Supplementary data to this article can be found online at https://doi.org/10.1016/j.soilbio.2021.108297.

References

Adkins, J., Jastrow, J.D., Morris, G.P., De Graaff, M.-A., 2019. Effects of fertilization, plant species, and intra-specific diversity on soil carbon and nitrogen in biofuel cropping systems after five growing seasons. Biomass and Bioenergy 130.
Bearden, B.N., 2001. Influence of arbuscular mycorrhizal fungi on soil structure and soil water characteristics of vertisols. Plant and Soil 229, 245–258.
Bodner, G., Leitner, D., Kaul, H.P., 2014. Coarse and fine root plants affect pore size distributions differently. Plant and Soil 380, 133–151.
Carminati, A., Vetterlein, D., Koebernick, N., Blaser, S., Weller, U., Vogel, H.J., 2013. Do roots mind the gap? Plant and Soil 367, 651–661.
Carrillo, Y., Bell, C., Koyama, A., Canarini, A., Boot, C.M., Wallenstein, M., Pendall, E., 2017. Plant traits, stoichiometry and microbes as drivers of decomposition in the rhizosphere in a temperate grassland. Journal of Ecology 105, 1750–1765.
Chatterjee, A., Long, D.S., Pierce, F.J., 2018. Change in soil organic carbon after five years of continuous winter wheat or switchgrass. Soil Science Society of America Journal 82, 332–342.
Chen, X.L., Chen, H.Y.H., Chen, C., Ma, Z.L., Searle, E.B., Yu, Z.P., Huang, Z.Q., 2020. Effects of plant diversity on soil carbon in diverse ecosystems: a global meta-analysis. Biological Reviews 95, 167–183.
Chenu, C., 1989. Influence of a fungal polysaccharide, scleroglucan, on clay microstructures. Soil Biology and Biochemistry 21, 299–305.
Chenu, C., Cosentino, D., 2011. Microbial regulation of soil structural dynamics. In: Ritz, K., Young, I. (Eds.), Architecture and Biology of Soils: Life in Inner Space. CABI, pp. 37–70.
Chimento, C., Almagro, M., Amaducci, S., 2016. Carbon sequestration potential in perennial bioenergy crops: the importance of organic matter inputs and its physical protection. Global Change Biology Bioenergy 8, 111–121.
Cong, W.F., van Ruijven, J., Mommer, L., De Deyn, G.B., Berendse, F., Hoffland, E., 2014. Plant species richness promotes soil carbon and nitrogen stocks in grasslands without legumes. Journal of Ecology 102, 1163–1170.
Cong, W.F., van Ruijven, J., van der Werf, W., De Deyn, G.B., Mommer, L., Berendse, F., Hoffland, E., 2015. Plant species richness leaves a legacy of enhanced root litter-induced decomposition in soil. Soil Biology and Biochemistry 80, 341–348.
Dawud, S.M., Raulund-Rasmussen, K., Ratcliffe, S., Domisch, T., Finer, L., Joly, F.-X., Hattenschwiler, S., Vesterdal, L., 2017. Tree species functional group is a more important driver of soil properties than tree species diversity across major European forest types. Functional Ecology 31, 1153–1162.

De Deyn, G.B., Quirk, H., Yi, Z., Oakley, S., Ostle, N.J., Bardgett, R.D., 2009. Vegetation composition promotes carbon and nitrogen storage in model grassland communities of contrasting soil fertility. Journal of Ecology 97, 864–875.
De Deyn, G.B., Shiel, R.S., Ostle, N.J., McNamara, N.P., Oakley, S., Young, I., Freeman, C., Fenner, N., Quirk, H., Bardgett, R.D., 2011. Additional carbon sequestration benefits of grassland diversity restoration. Journal of Applied Ecology 48, 600–608.
De Gryze, S., Jassogne, L., Six, J., Bossuyt, H., Wevers, M., MerckX, R., 2006. Pore structure changes during decomposition of fresh residue: X-ray tomography analyses. Geoderma 134, 82–96.
Dorioz, J.M., Robert, M., Chenu, C., 1993. The role of roots, fungi, and bacteria on clay particle organization - an experimental approach. Geoderma 56, 179–194.
Doube, M., Klosowski, M.M., Arganda-Carreras, I., Cordelieres, F.P., Dougherty, R.P., Jackson, J.S., Schmid, B., Hutchinson, J.R., Shefelbine, S.J., 2010. BoneJ Free and extensible bone image analysis in ImageJ. Bone 47, 1076–1079.
Emerson, W.W., McGarry, D., 2003. Organic carbon and soil porosity. Australian Journal of Soil Research 41, 107–118.
Emery, S.M., Kinnetz, E.R., Bell-Dereske, L., Stahlheber, K.A., Gross, K.L., Pennington, D., 2018. Low variation in arbuscular mycorrhizal fungal associations and effects on biomass among switchgrass cultivars. Biomass and Bioenergy 119, 503–508.
Feeney, D.S., Crawford, J.W., Daniell, T., Hallett, P.D., Nunan, N., Ritz, K., Rivers, M., Young, I.M., 2006. Three-dimensional microorganization of the soil-root-microbe system. Microbial Ecology 52, 151–158.
Fischer, H., Ingwersen, J., Kuzyakov, Y., 2010. Microbial uptake of low-molecular-weight organic substances out-competes sorption in soil. European Journal of Soil Science 61, 504–513.
Fornara, D.A., Tilman, D., 2008. Plant functional composition influences rates of soil carbon and nitrogen accumulation. Journal of Ecology 96, 314–322.
Francis, R., Read, D.J., 1984. Direct transfer of carbon between plants connected by vesicular arbuscular mycorrhizal mycelium. Nature 307, 53–56.
Gahoonia, T.S., Care, D., Nielsen, N.E., 1997. Root hairs and phosphorus acquisition of wheat and barley cultivars. Plant and Soil 191, 181–188.
Grierson, C., Nielsen, E., Ketelaarc, T., Schiefelbein, J., 2014. Root Hairs, vol. 12. The arabidopsis book, p. e0172 e0172.
Helliwell, J.R., Sturrock, C.J., Mairhofer, S., Craigon, J., Ashton, R.W., Miller, A.J., Whalley, W.R., Mooney, S.J., 2017. The emergent rhizosphere: imaging the development of the porous architecture at the root-soil interface. Scientific Reports 7.
Helliwell, J.R., Sturrock, C.J., Miller, A.J., Whalley, W.R., Mooney, S.J., 2019. The role of plant species and soil condition in the structural development of the rhizosphere. Plant, Cell and Environment 42, 1974–1986.
Horn, R., Taubner, H., Wuttke, M., Baumgartl, T., 1994. Soil physical properties related to soil structure. Soil and Tillage Research 30, 187–216.
IPCC, 2018. Global warming of 1.5 °C. An IPCC special report on the impacts of global warming of 1.5°C above pre-industrial levels and related global greenhouse gas emission pathways. In: Change, I.P.o.C. (Ed.), The Context of Strengthening the Global Response to the Threat of Climate Change, Sustainable Development, and Efforts to Eradicate Poverty.
Jach-Smith, L.C., Jackson, R.D., 2018. N addition undermines N supplied by arbuscular mycorrhizal fungi to native perennial grasses. Soil Biology and Biochemistry 116, 148–157.
Jach-Smith, L.C., Jackson, R.D., 2020. Inorganic N addition replaces N supplied to switchgrass (Panicum virgatum) by arbuscular mycorrhizal fungi. Ecological Applications 30.
Johnson, N.C., Wilson, G.W.T., Wilson, J.A., Miller, R.M., Bowker, M.A., 2015. Mycorrhizal phenotypes and the law of the minimum. New Phytologist 205, 1473–1484.
Jones, D.L., Kemmitt, S.J., Wright, D., Cuttle, S.P., Bol, R., Edwards, A.C., 2005. Rapid intrinsic rates of amino acid biodegradation in soils are unaffected by agricultural management strategy. Soil Biology and Biochemistry 37, 1267–1275.
Jones, D.L., Nguyen, C., Finlay, R.D., 2009. Carbon flow in the rhizosphere: carbon trading at the soil-root interface. Plant and Soil 321, 5–33.
Kaiser, C., Kilburn, M.R., Clode, P.L., Fuchslueger, L., Koranda, M., Cliff, J.B., Solaiman, Z.M., Murphy, D.V., 2015. Exploring the transfer of recent plant photosynthates to soil microbes: mycorrhizal pathway vs direct root exudation. New Phytologist 205, 1537–1551.
Kantola, I.B., Masters, M.D., DeLucia, E.H., 2017. Soil particulate organic matter increases under perennial bioenergy crop agriculture. Soil Biology and Biochemistry 113, 184–191.
Kapur, J, Sahoo, P, Wong, A, 1985. A new method for gray-level picture thresholding using the entropy of the histogram. Computer vision, graphics, and image processing 29 (3), 273–285. https://doi.org/10.1016/0734-189X(85)90125-2.
Kravchenko, A.N., Guber, A.K., Rasavi, B.S., Koestel, J., Quigley, M.Y., Robertson, G.P., Kuzyakov, Y., 2019. Microbial spatial footprint as a driver of soil carbon stabilization. Nature Communications 10.
Lange, M., Eisenhauer, N., Sierra, C.A., Bessler, H., Engels, C., Griffiths, R.I., Mellado-Vazquez, P.G., Malik, A.A., Roy, J., Scheu, S., Steinbeiss, S., Thomson, B.C., Trumbore, S.E., Gleixner, G., 2015. Plant diversity increases soil microbial activity and soil carbon storage. Nature Communications 6.
Leifheit, E.F., Veresoglou, S.D., Lehmann, A., Morris, E.K., Rillig, M.C., 2014. Multiple factors influence the role of arbuscular mycorrhizal fungi in soil aggregation-a meta-analysis. Plant and Soil 374, 523–537.
Loeppmann, S., Forbush, K., Cheng, W., Pausch, J., 2019. Subsoil biogeochemical properties induce shifts in carbon allocation pattern and soil C dynamics in wheat. Plant and Soil 442, 369–383.
Mahaney, W.M., Smemo, K.A., Gross, K.L., 2008. Impacts of C(4) grass introductions on soil carbon and nitrogen cycling in C(3)-dominated successional systems. Oecologia 157, 295–305.
Materechera, S.A., Dexter, A.R., Alston, A.M., 1992. Formation of aggregates by plant-roots in homogenized soils. Plant and Soil 142, 69–79.
McLaughlin, S.B., Kszos, L.A., 2005. Development of switchgrass (Panicum virgatum) as a bioenergy feedstock in the United States. Biomass and Bioenergy 28, 515–535.
Meding, S.M., Zasoski, R.J., 2008. Hyphal-mediated transfer of nitrate, arsenic, cesium, rubidium, and strontium between arbuscular mycorrhizal forbs and grasses from a California oak woodland. Soil Biology and Biochemistry 40, 126–134.
Milleret, R., Le Bayon, R.C., Lamy, F., Gobat, J.M., Boivin, P., 2009. Impact of roots, mycorrhizas and earthworms on soil physical properties as assessed by shrinkage analysis. Journal of Hydrology 373, 499–507.
Milliken, G.A., Johnson, D.E., 2009. Analysis of Messy Data Volume I: Designed Experiments, second ed. CRC Press.
Minasny, B., Malone, B.P., McBratney, A.B., Angers, D.A., Arrouays, D., Chambers, A., Chaplot, V., Chen, Z.S., Cheng, K., Das, B.S., Field, D.J., Gimona, A., Hedley, C.B., Hong, S.Y., Mandal, B., Marchant, B.P., Martin, M., McConkey, B.G., Mulder, V.L., O'Rourke, S., Richer-de-Forges, A.C., Odeh, I., Padarian, J., Paustian, K., Pan, G.X., Poggio, L., Savin, I., Stolbovoy, V., Stockmann, U., Sulaeman, Y., Tsui, C.C., Vagen, T.G., van Wesemael, B., Winowiecki, L., 2017. Soil carbon 4 per mille. Geoderma 292, 59–86.
Montesinos-Navarro, A., Verdu, M., Ignacio Querejeta, J., Valiente-Banuet, A., 2017. Nurse plants transfer more nitrogen to distantly related species. Ecology 98, 1300–1310.
Moran-Zuloaga, D., Dippold, M., Glaser, B., Kuzyakov, Y., 2015. Organic nitrogen uptake by plants: reevaluation by position-specific labeling of amino acids. Biogeochemistry 125, 359–374.
Munch, B., Holzer, L., 2008. Contradicting geometrical concepts in pore size analysis attained with electron microscopy and mercury intrusion. Journal of the American Ceramic Society 91, 4059–4067.
Naveed, M., Brown, L.K., Raffan, A.C., George, T.S., Bengough, A.G., Roose, T., Sinclair, I., Koebernick, N., Cooper, L., Hackett, C.A., Hallett, P.D., 2017. Plant exudates may stabilize or weaken soil depending on species, origin and time. European Journal of Soil Science 68, 806–816.
Newman, E.I., Ritz, K., 1986. Evidence on the pathways of phosphorus transfer between vesicular-arbuscular mycorrhizal plants. New Phytologist 104, 77–87.
Pausch, J., Zhu, B., Kuzyakov, Y., Cheng, W.X., 2013. Plant inter-species effects on rhizosphere priming of soil organic matter decomposition. Soil Biology and Biochemistry 57, 91–99.
Philip, L., Simard, S., Jones, M., 2010. Pathways for below-ground carbon transfer between paper birch and Douglas-fir seedlings. Plant Ecology & Diversity 3, 221–233.
Poirier, V., Roumet, C., Munson, A.D., 2018. The root of the matter: linking root traits and soil organic matter stabilization processes. Soil Biology and Biochemistry 120, 246–259.
Rasband, W.S., 1997-2015. ImageJ. U.S. National Institutes of Health, Bethesda, MD, USA.
Remus, R., Augustin, J., 2016. Dynamic linking of C-14 partitioning with shoot growth allows a precise determination of plant-derived C input to soil. Plant and Soil 408, 493–513.
Rillig, M.C., Mummey, D.L., 2006. Mycorrhizas and soil structure. New Phytologist 171, 41–53.
Rillig, M.C., Wright, S.F., Allen, M.F., Field, C.B., 1999. Rise in carbon dioxide changes in soil structure. Nature 400, 628, 628.
Roley, S.S., Duncan, D.S., Liang, D., Garoutte, A., Jackson, R.D., Tiedje, J.M., Robertson, G.P., 2018. Associative nitrogen fixation (ANF) in switchgrass (Panicum virgatum) across a nitrogen input gradient. PloS One 13.
Sanaullah, M., Chabbi, A., Rumpel, C., Kuzyakov, Y., 2012. Carbon allocation in grassland communities under drought stress followed by C-14 pulse labeling. Soil Biology and Biochemistry 55, 132–139.
Schenk, H.J., 2006. Root competition: beyond resource depletion. Journal of Ecology 94, 725–739.
Simard, S.W., Beiler, K.J., Bingham, M.A., Deslippe, J.R., Philip, L.J., Teste, F.P., 2012. Mycorrhizal networks: mechanisms, ecology and modelling. Fungal Biology Reviews 26, 39–60.
Simard, S.W., Perry, D.A., Jones, M.D., Myrold, D.D., Durall, D.M., Molina, R., 1997. Net transfer of carbon between ectomycorrhizal tree species in the field. Nature 388, 579–582.
Six, J., Elliott, E.T., Paustian, K., 2000. Soil macroaggregate turnover and microaggregate formation: a mechanism for C sequestration under no-tillage agriculture. Soil Biology and Biochemistry 32, 2099–2103.
Smercina, D.N., Evans, S.E., Friesen, M.L., Tiemann, L.K., 2019. To fix or not to fix: controls on free-living nitrogen fixation in the rhizosphere. Applied and Environmental Microbiology 85.
Smith, S.E., Smith, F.A., 2011. Roles of arbuscular mycorrhizas in plant nutrition and growth: new paradigms from cellular to ecosystem scales. Annual Review of Plant Biology 62, 227–250.
Sprunger, C.D., Robertson, G.P., 2018. Early accumulation of active fraction soil carbon in newly established cellulosic biofuel systems. Geoderma 318, 42–51.
Staddon, P.L., Ramsey, C.B., Ostle, N., Ineson, P., Fitter, A.H., 2003. Rapid turnover of hyphae of mycorrhizal fungi determined by AMS microanalysis of C-14. Science 300, 1138–1140.
Steinbeiss, S., Bessler, H., Engels, C., Temperton, V.M., Buchmann, N., Roscher, C., Kreutziger, Y., Baade, J., Habekost, M., Gleixner, G., 2008. Plant diversity positively

affects short-term soil carbon storage in experimental grasslands. Global Change Biology 14, 2937–2949.
Strong, D.T., De Wever, H., Merckx, R., Recous, S., 2004. Spatial location of carbon decomposition in the soil pore system. European Journal of Soil Science 55, 739–750.
Stroup, W.W., Milliken, G.A., Claassen, E.A., Wolfinger, R.D., 2018. SAS for Mixed Models: Introduction and Basic Applications. SAS Institute Inc., Cary, NC, USA.
Sun, Y., Zang, H., Splettstosser, T., Kumar, A., Xu, X., Kuzyakov, Y., Pausch, J., 2020. Plant Intraspecific Competition and Growth Stage Alter Carbon and Nitrogen Mineralization in the Rhizosphere. Plant Cell and Environment.
Tilman, D., Wedin, D., Knops, J., 1996. Productivity and sustainability influenced by biodiversity in grassland ecosystems. Nature 379, 718–720.
Tisdall, J.M., Oades, J.M., 1982. Organic matter and water stable aggregates in soils. Journal of Soil Science 33, 141–163.
van der Heijden, M.G.A., Klironomos, J.N., Ursic, M., Moutoglis, P., Streitwolf-Engel, R., Boller, T., Wiemken, A., Sanders, I.R., 1999. Sampling effect", a problem in biodiversity manipulation? A reply to David A. Wardle. Oikos 87, 408–410.
Walter, L.E.F., Hartnett, D.C., Hetrick, B.A.D., Schwab, A.P., 1996. Interspecific nutrient transfer in a tallgrass prairie plant community. American Journal of Botany 83, 180–184.
Weaver, R.W., Wright, S.F., Varanka, M.W., Smith, O.E., Holt, E.C., 1980. Dinitrogen fixation (C2H2) by established forage grasses in Texas. Agronomy Journal 72, 965–968.
Wilson, G.W.T., Rice, C.W., Rillig, M.C., Springer, A., Hartnett, D.C., 2009. Soil aggregation and carbon sequestration are tightly correlated with the abundance of arbuscular mycorrhizal fungi: results from long-term field experiments. Ecology Letters 12, 452–461.
Yang, Y., Tilman, D., Furey, G., Lehman, C., 2019. Soil carbon sequestration accelerated by restoration of grassland biodiversity. Nature Communications 10.

Supporting information

Figure S1. Greenhouse experiment set-up: a) Schematic representation of the experimental setup where unlabeled plants were kept in light impenetrable bags during labeling events; b) Labeling chambers with unlabeled plants covered by light-impenetrable bags; c) Schematic representation of an experimental pot marking the locations of intact soil cores that were used for µCT pore characterization.

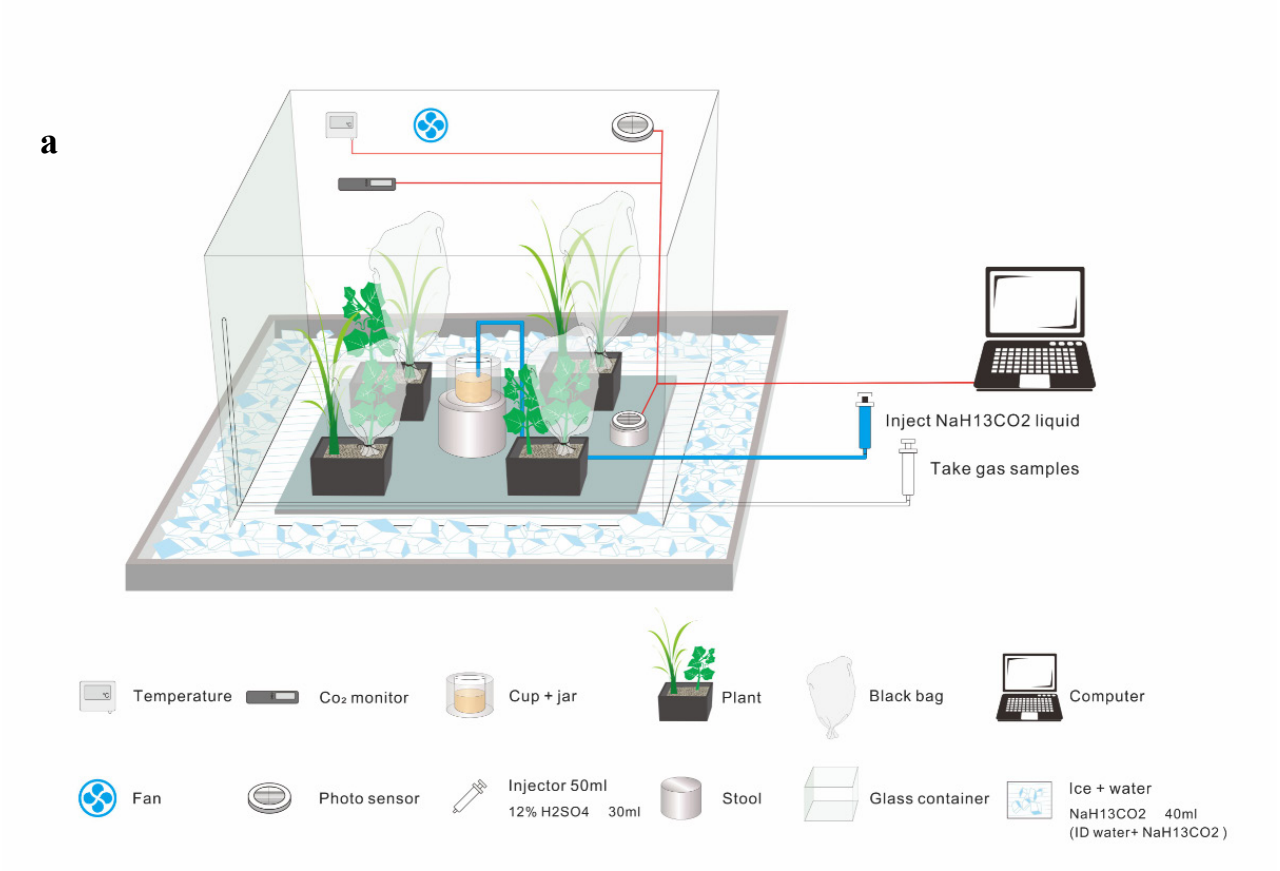

b

c

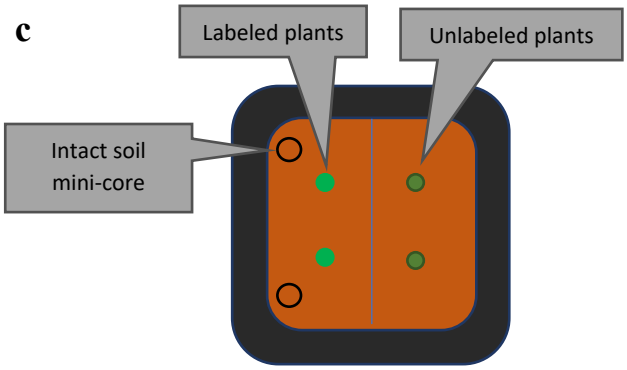

Figure S2. (a) Sample histogram of gray-scale values from computed micro-tomography image of one of the studied micro-cores. Arrows show the ranges of grays-scale values that were used in thresholding stone/sand particles, pores, and plant roots. (b) Sample gray-scale image of one of the micro-cores. Shown are original image (left), the image with initial thresholding applied to the root with green and yellow arrows pointing to the root and the thresholding artefacts (middle), and the image with outlined root segment that will be used in subsequent analyses (green) and stones/sand particles (pink) (right).

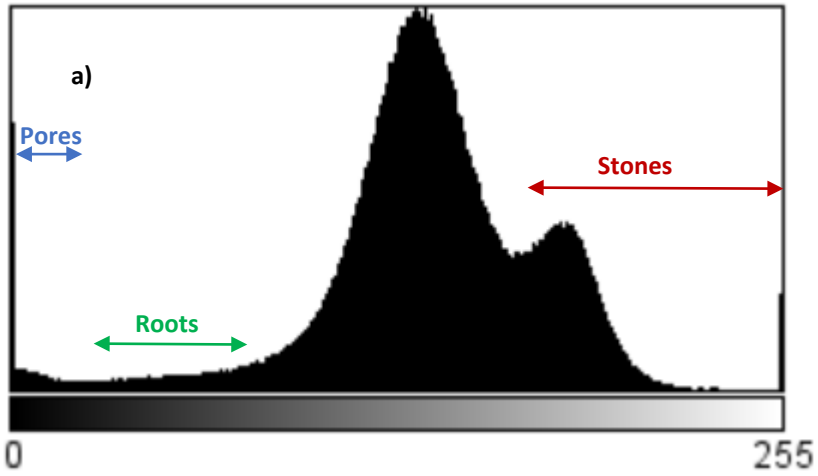

b)

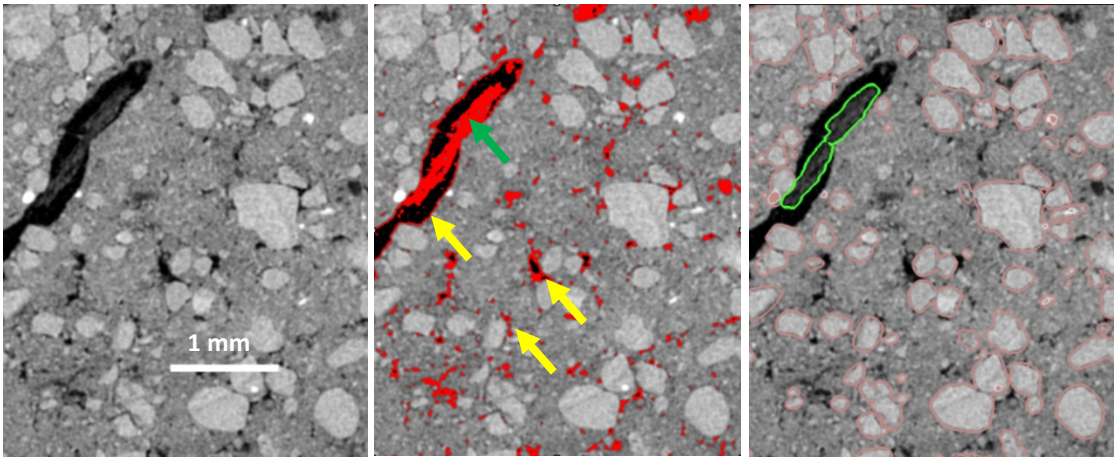

Figure S3. Plant biomass (a) aboveground and (b) belowground for the labeled (source) plants. X-axis represents the monoculture and polyculture plant systems; they are the plant species for which the biomass is reported (SW-switchgrass, BB- big blue stem, WB - wild bergamot). Color represent the other species with which plants grew in intercropped systems. Shown are means (crosses), standard errors (vertical lines), and original data points. Letters mark significant differences among the plant systems, ** mark the differences among the species within each system ($p<0.05$, t-tests).

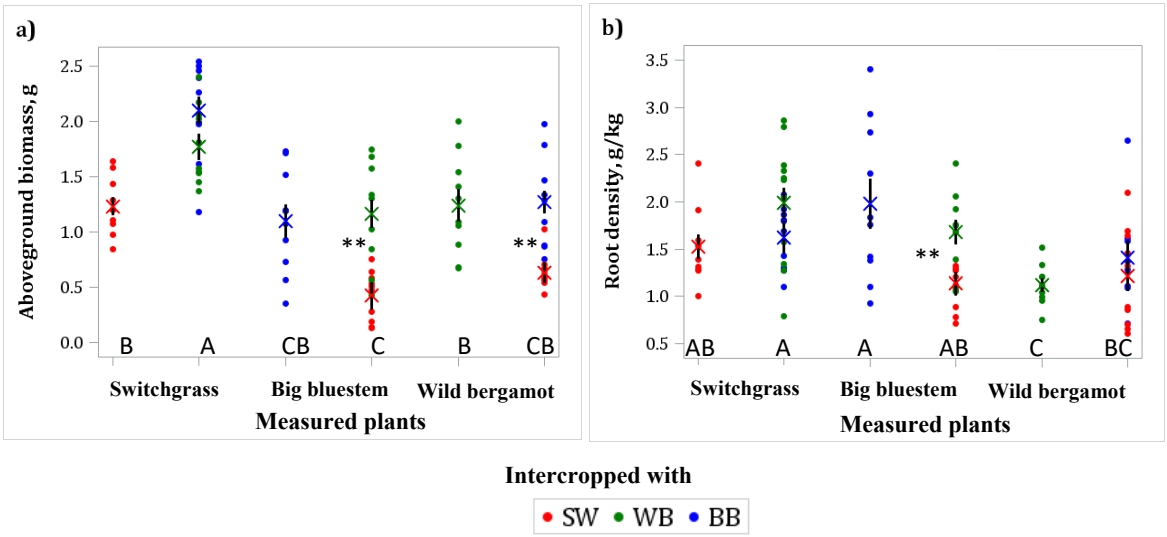

Figure S4. $\delta^{13}C$ in (a) above and (b) below plant biomass of the labeled (source) plants and in soil (c). X-axis represents the monoculture and polyculture plant systems; they are the plant species for which the biomass is reported (SW-switchgrass, BB- big blue stem, WB - wild bergamot). Color represent the other species with which plants grew in polyculture systems. Shown are means (crosses), standard errors (vertical lines), and original data points (n=5). Letters mark significant differences among the three plant system treatments within each plant species, NS means that the three plant system treatments were not significantly different from each other ($p<0.05$ for a) and b), $p<0.1$ for c), t-tests).

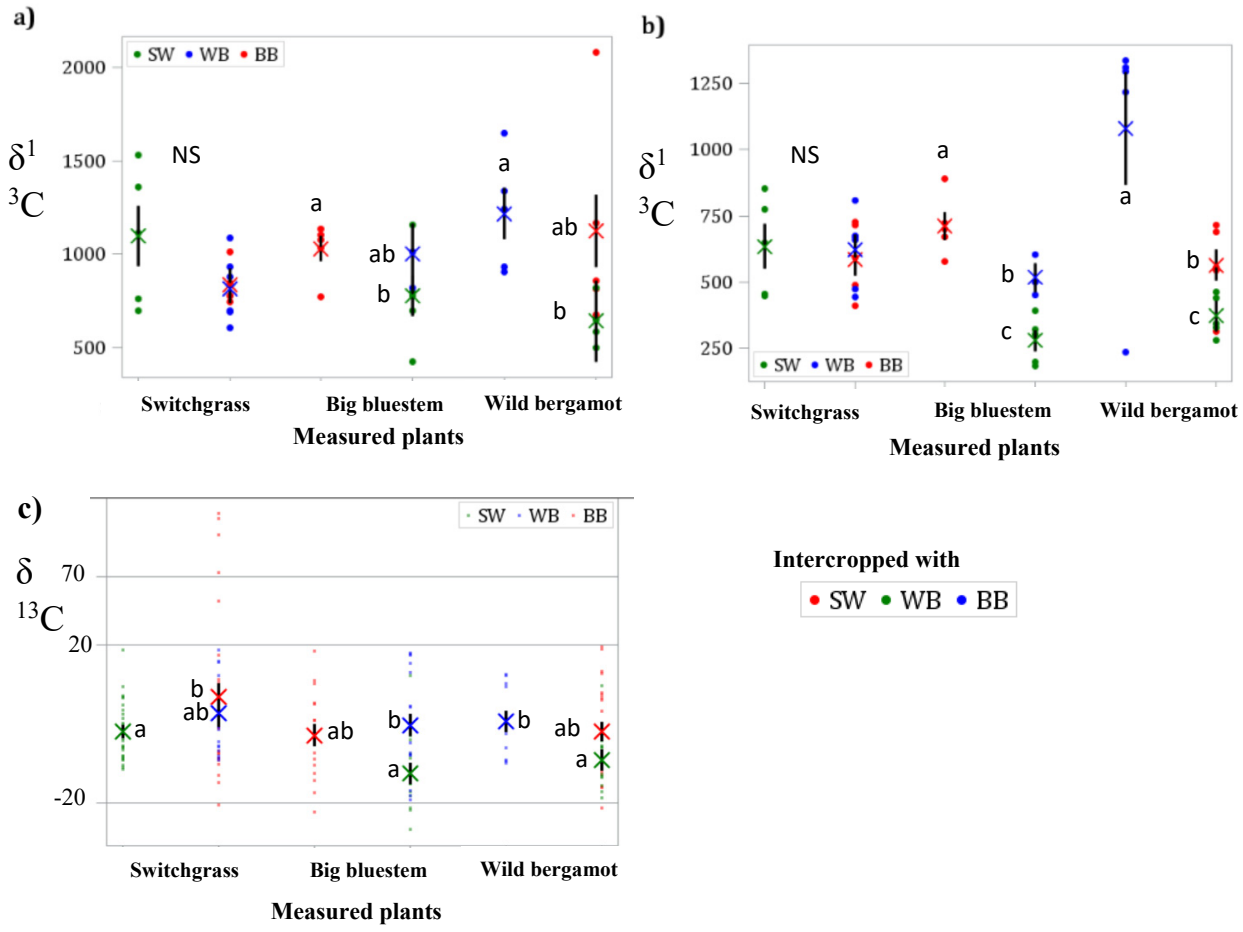

Figure S5. Soil $\delta^{13}C$ values of the plant systems plotted as a function of the total ^{13}C in the roots of the labeled plants. Shown are averages (n=5). Yellow dash line marks the unplanted control soil. ** mark the R^2 significant at $p<0.05$, shaded area represents 95% confidence intervals for the mean.